35th Annual International Conference of the IEEE EMBS
Osaka, Japan, 3 - 7 July, 2013

A Two-stage Reconstruction of Fluorescence Molecular Tomography Based on Sparse Regularization

Jingxing Cheng, Yuqing Hou, Jingjing Yu, and Xiaowei He*

Abstract—**Fluorescence molecular tomography (FMT) is a promising imaging modality that offers the possibilities to monitor cellular and molecular function in vivo. However, accurate and stable reconstruction of fluorescence-labeled targets remains a challenging problem. In this contribution, a two-stage reconstruction algorithm that combines sparse regularization with adaptive finite element method is proposed, and two different inversion algorithms are employed separately on the initial coarse mesh and the second refined one. Numerical experiment results with a digital mouse model demonstrate the stability and computational efficiency of the proposed method for FMT.**

I. Introduction

Optical molecular imaging of small animal has been extensively applied in preclinical research. Compared to planar fluorescence reflectance imaging, three-dimensional tomography tends to provide more accurate and quantitative biological information to facilitate monitoring biological function particularly in terms of disease progression and drug efficacy [1-3]. Therefore, fluorescence molecular tomography (FMT), aiming at localization and quantification of fluorescence probes, have drawn great attention and witnessed a rapid development in recent years.

The reconstruction problem involved in this paper is solely to recover fluorescent probe concentration. Generally, one can figure out the distribution of fluorescent target by minimizing the misfit between the boundary intensity measurements and the measurements predicted with a forward model. For example, the photon propagation within biological tissue can be well depicted using the steady diffusion approximation model of radiative transfer equation, i.e. steady diffusion equation. By neglecting the change in optical properties of the medium (absorption and scattering), the corresponding forward model comes down to a linear equation and the reconstruction is typically achieved by inverse techniques. Since there are a large number of unknowns that need to be resolved from very limited boundary measurements, the inverse problem of FMT is highly ill-posed [4,5]. Therefore, accurate and stable reconstruction of fluorescence-labeled targets remains a challenge.

In order to obtain a stable approximate solution and improve the imaging quality, some additional prior information should be incorporated to regularize the FMT inverse problem, such as anatomical structure, local smoothness, and so on [4]. And a variety of methods that include regularization have been presented for linear reconstruction in FMT. Among them, Tikhonov regularization is an l_2-norm method that can be solved efficiently by standard minimization algorithms, but tends to produce over-smoothed solution [5].

In view of the fact that most of the mechanisms studied with FMT occur in very localized regions, some l_p ($1 \leqslant p < 2$) norm based sparse regularization methods have recently drawn considerable amount of attention in FMT [5,6]. In these reports, a typical way of exploiting the sparsity constraint is to replace the l_2-norm regularizer in Tikhonov method with l_1-norm one. And then sophisticated algorithm is applied to solve the convex optimal problem.

Recently, a hybrid reconstruction based on the *hp*-finite element method has been proposed for FMT to improve the stability of the solution [7]. It involves a multi-level reconstruction process, i.e. sparsity regularization is applied to the first coarse mesh level, and Landweber iterative regularization is adopted on the subsequent refined meshes. The simulation experiments show the potential and feasibility of the hybrid approach (hereinafter to be referred as ITCG_Land), but the accuracy of the reconstruction needs further improvement.

In this contribution, we propose a two-stage optimization algorithm for linear reconstruction in FMT. By using the sparsity as a cue for finding the correct solution, fluorescent concentration is recovered via solving two l_1-norm minimization problems. In the first stage, an approximate message passing (AMP) algorithm was applied to a coarse finite element mesh, which produces an initial solution [8]. After that, a local region is determined and refined according to the obtained initial solution, and the fluorescent concentration is finally recovered by solving a small scale optimization problem with primal augmented Lagrangian method (PALM) in the second stage [9]. The proposed algorithm is referred as AMP_PALM in the following parts of this article.

This work is supported by the National Basic Research Program of China (973 Program) under Grant No. 2011CB311802, the Specialized Research Fund for the Doctoral Program of Higher Education of China (New Teachers) under Grant No.20116101120018, the China Postdoctoral Science Foundation funded project under Grant Nos. 2011M501467 and 2012T50814, the Natural Science Basic Research Plan in Shaanxi Province of China under Grant Nos. 2011JQ8029 and 2011JQ1006, the Science and Technology Plan Program in Shaanxi Province of China (New Scientific and Technological Star) under Grant No. 2012KJXX-29, the Fundamental Research Funds for the Central Universities, the Graduate Innovation Project of Northwest University under Grant No.YZZ12093, and the Science and Technology Program of Educational Committee of Shaanxi Province of China under Grant No.12JK0729.

J. Cheng, Y. Hou, and X. He are with the School of Information Sciences and Technology, Northwest University, Xi'an, 710069, China. (phone: 86-29-8830-8161; fax: 86-29-8830-8161; e-mail: hexw@ nwu.edu.cn).

J. Yu is with School of Physics and Information Technology, Shaanxi Normal University, Xi'an, 710062, China (e-mail: yujj@snnu.edu.cn).

II. METHOD

A. The inverse model of FMT

Based on the diffusion equation and Robin-type boundary conditions, the matrix form of the relationship between the measured photon flux density Φ and the fluorescent yield X is derived with the finite element method [11-13]:

$$\Phi = AX \tag{1}$$

where system matrix $A \in R^{m \times n} (m << n)$ is usually ill-conditioned.

As mentioned above, most of the mechanisms studied with FMT happen in localized regions, which means that the fluorescent targets to be recovered are usually very small and sparse compared with the entire reconstruction domain [6]. Moreover, the sparsity-promoting property of l_1-norm regularization has been shown in many areas of optical tomography [13]. Consequently, according sparse signal recovery framework, the unknown fluorescent concentration can be well approximated by the solution of the following l_1-norm minimization problem:

$$\min_X \left\{ \left\| \Phi - AX \right\|_2^2 + \lambda \left\| X \right\|_1 \right\} \tag{2}$$

where $\left\| X \right\| = \sum_i |x_i|$ and λ is a regularization parameter.

B. Two-stage Reconstruction

In optical tomography adaptive finite element method (AFEM) is a good tradeoff between image resolution and stabilization of the inverse problem [5]. The two stage reconstruction present in this paper is developed based on the adaptive finite element method. However, the proposed method is different from the previous AFEM methods that use one inversion algorithm on different mesh levels. The reconstruction process is divided into two related stages with different discretization levels, and the difference between the former and the latter mesh is also taken into account.

In the first stage, the domain is discretized into a uniformly coarse mesh to maintain the computational economy. To obtain an initial solution, AMP algorithm is exploited to solve the objective function on the coarse mesh. AMP is a fast and simple costless modification to iterative thresholding, inspired by belief propagation framework in graphical models [14]. Following the graph-theoretic framework, the reconstruction problem of FMT is modeled by a factor graph $G = \{X, M, N\}$. Here G is a complete bipartite graph with variable nodes $X=\{X_1, X_2, \cdots, X_n\}$, factor nodes $M=\{m_1, m_2, \cdots, m_n\}$, and edges $N = X \times M = \{(X_i, m_j) \,|\, X_i \in X, m_j \in M\}$. Assuming that the probability distribution of each variable X_i satisfies a Laplace prior $\frac{1}{z}\exp(-\alpha |X_i|)$, and every factor node m_j is a Dirac delta function $\delta\left(\Phi_j = (AX)_j\right)$, then the joint probability distribution for the vector Φ and solution X is the following function:

$$p(\Phi, X) = \frac{1}{z} \prod_{i=1}^{n} \exp(-\alpha |X_i|) \prod_{j=1}^{m} \delta\left(\Phi_j = (AX)_j\right) \tag{3}$$

When $\alpha \to \infty$, the joint probability $p(\Phi, X)$ will concentrate around the sparse solution of Equation (2). In this model, every function m_j ensures the solution satisfies the constraint $\Phi = AX$. Therefore, the fluorescent yield can be estimated by iteratively computing the marginal distribution $p(X_i)$ for each given variable X_i.

Although the solution in this step is not accurate enough due to the coarse mesh, it still indicates the potential region around real targets. Hence, after the first round inversion completes, adaptive mesh refinement starts. All of the entries with nonzero reconstructed value are selected to be refined using the longest-edge bisection method. Thus, a locally refined mesh is obtained, keeping fine resolution in region of interest and coarser resolution in other regions.

In the second stage, the size of the minimization problem apparently diminishes, because the solution space is constrained to the refined region. Another first-order method for solving Equation (2), the PALM algorithm, is applied to the recover the fluorescent target. Specifically, the objective function in Equation (2) is reformulated to the following form with an additional penalty term:

$$\min_X \left\{ \Gamma_\eta(X, \theta) = \left\| X \right\|_1 + \frac{\eta}{2} \left\| \Phi - AX \right\|_2^2 + \theta^T (\Phi - AX) \right\} \tag{4}$$

where η is the regularization parameter, θ is a vector of Lagrangian multipliers. Finally, the solution is determined by computing X and θ iteratively:

$$\begin{cases} X_{k+1} = \arg\min_X \Gamma_\eta(X, \theta_k) \\ \theta_{k+1} = \theta_k + \eta(\Phi - AX) \end{cases} \tag{5}$$

where the subproblem for X is solved via a fast iterative soft-thresholding algorithm . The interested reader is referred to for more details of PALM algorithm in [9].

III. EXPERIMENTS AND RESULTS

A. 3D digital mouse model

In this section, we evaluate the performance and effectiveness of the proposed two-stage reconstruction method with a group of numerical experiments.

In the following experiments, we utilize the same digital mouse model as in [7] for comparison purposes. The 3D digital mouse atlas of CT and cryosection data was utilized to provide anatomical information. And only the torso section of the mouse model with a height of 35mm was selected as the region to be investigated. A cylindrical fluorescent target with 0.8 mm radius and 1.6 mm height locates in the liver with center at (11.9mm, 6.4mm, 16.4mm), as shown in Figure 1. And the fluorescent concentration of the target is set as 0.05mm^{-1}. The optical parameters of different organs are listed in Table I [7].

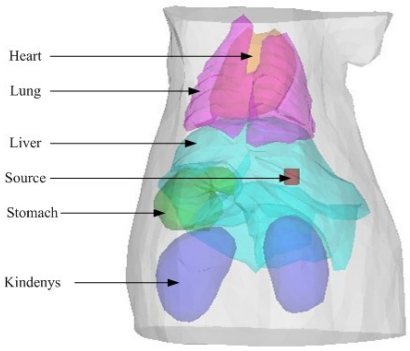

Figure 1. The torso of the mouse mode with a cylindrical fluorescent target in the liver.

TABLE I. OPTICAL PROPERTIES FOR THE ATLAS ORGANS REGION

Material	$\mu_{ax}\ (mm^{-1})$	$\mu'_{sx}\ (mm^{-1})$	$\mu_{am}\ (mm^{-1})$	$\mu'_{sm}\ (mm^{-1})$
Heart	0.0083	1.01	0.0104	0.99
Lungs	0.0133	1.97	0.0203	1.95
Liver	0.0329	0.70	0.0176	0.65
Stomach	0.0114	1.74	0.0070	1.36
Kidneys	0.0660	2.25	0.0380	2.02
Muscle	0.0052	1.08	0.0068	1.03

B. Source Reconstruction

The simulated measurements were generated by solving the forward model with FEM. Specifically, the torso model of mouse was discretized into 132,202 tetrahedral elements and 24,906 nodes. And the fluorescent target was excited by 18 point sources at different positions in sequence.

In the first-stage reconstruction, the maximum mesh size was conditioned as 2.8mm. The model was discretized into 14,086 tetrahedral elements and 2954 nodes. Then the AMP algorithm was applied for the first round reconstruction on this initial coarse mesh. The regularization parameter was adjusted manually, ranging from 1e-7 to 1e-12.

In all of the experiments, the largest component of vector X was regarded as the reconstructed fluorescent yield, and the corresponding node were recognized as the center of the target.

The second-stage reconstruction was based on the first-stage solution. In our implementation, the elements with their values bigger than 70% of the maximum were selected for refinement. Additionally, the corresponding boundary elements were also selected to be divided with the longest refinement method.

In the first set of experiments, we compared the reconstruction results by the AMP_PALM, ITCG_Land, and L1LS_L1LS. Here L1LS_L1LS means the L1LS algorithm [14] is applied twice in succession on the different mesh levels. The quality of the reconstruction is quantitatively evaluated with location error and reconstructed fluorescent yield. Location error is the distance between the centers of the reconstructed target and the actual one. The quantitative comparisons between them are presented in Table II. Figure 2 shows the reconstruction results of the above three methods in the form of 3D iso-surface.

TABLE II. RESULTS FOR SOURCE RECONSTRUCTION

Method	Position Center (mm)	Location Error (mm)	Fluorescent Yield (mm^{-1})
AMP_PALM	**12.4,6.8,16.6**	**0.660**	**0.00122**
ITCG_Land	11.5,6.6,15.4	1.048	0.00117
L1LS_L1LS	11.5,6.9,15.5	1.049	0.00025

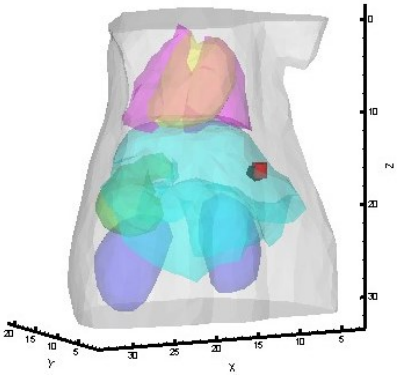

(a) AMP PALM

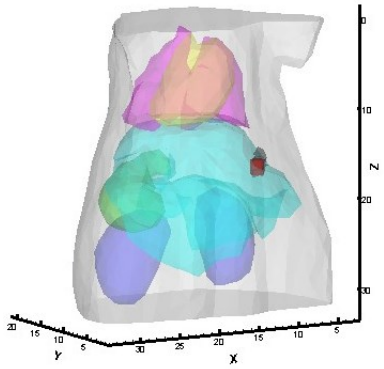

(b) ITCG Land

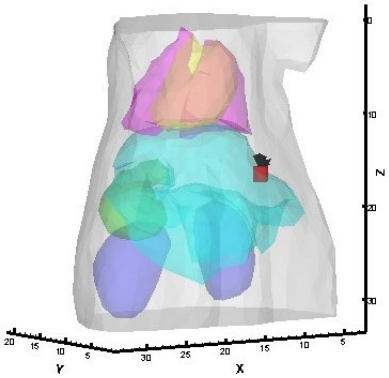

(c) L1LS_L1LS

Figure 2. 3D Reconstuction results for a single fluorescent target by the proposed AMP_PALM, ITCG_Land, and L1LS_L1LS method.

From Table II, we observe that AMP_PALM is the best algorithm followed by ITCG_Land. As for the location accuracy, the two-stage method produced the most accurate result with an error of 0.66 mm. In contrast, the location errors for the other two methods are almost doubled. Additionally, the fluorescent yield of L1LS_L1LS method is obviously lower than AMP_PALM and ITCG_Land method. Compared to the actual fluorescent concentration, the relative deviation

of the reconstructed value by L1LS_L1LS method reaches up to 95%, whereas the relative error by AMP_PALM method reduces to 75%.

C. Stability Analysis

To evaluate the stability and robustness of the two-stage reconstruction algorithm, a group of experiments were conducted by adding different levels of Gaussian noise to simulated boundary measurements. For each noise level, we performed 100 independent reconstructions. The average result is summarized in Table III.

From Table III, we can obviously observe that the reconstructed location remain constant as the noise level increases. The fluorescent yield is not significantly affected by noise for all of the noise levels considered. The results show that the proposed two-stage reconstruction method is quite robust to measurement noise.

TABLE III. IMPACT OF NOISE ON THE PROPOSED METHOD

Noise level	Position Center (mm)	Location Error (mm)	Fluorescent Yield (mm^{-1})
0%	12.4,6.8,16.6	0.66	0.00122
10%	12.4,6.8,16.6	0.66	0.00123
20%	12.4,6.8,16.6	0.66	0.00121
30%	12.4,6.8,16.6	0.66	0.00123

IV. DISCUSSION AND CONCLUSION

In this paper, we report a two-stage reconstruction method for linear reconstruction problem in FMT. Taking the sparse distribution of fluorescent target into account, we take full use of sparse regularization to deal with the ill-posedness of FMT. Additionally, the proposed method combines the merit of adaptive FEM to to maintain stability and efficiency. The experiments with a mouse atlas model demonstrate that the two-stage method can provide satisfactory results in reconstruction quality and robustness.

As mentioned in section II, the two rounds of reconstruction are related. Since the second stage reconstruction is based on the solution of the first-stage, the inversion algorithm on the initial coarse mesh plays an important role in the whole reconstruction process. As an illustration, Table IV presents the comparison results by AMP, ITCG, and L1LS method on the first mesh level. As indicated in Table IV, the AMP algorithm performs best on this mesh level, both in term of location accuracy and fluorescent yield. Hence, it is reasonable that a better initial solution guides the subsequent reconstruction on finer meshes to yield more accurate quantitative results.

The two-stage reconstruction involves two distinct algorithms. AMP is a dramatically fast algorithm that has been verified by Donoho et al. in [8]. For PALM, the computational time is dominated by matrix-vector multiplication, whose complexity is $O(n^2)$, but the size of the matrix on the second mesh level has sharply decreased with the local refinement processing. Consequently, the two-stage reconstruction method is computational efficient, which is also evidenced in our experiment results. The AMP_PALM runs faster than its counterparts do.

TABLE IV. RESULTS WITH DIFFERENT METHODS ON FIRST MESH LEVEL

Method	Position Center (mm)	Location Error (mm)	Fluorescent Yield (mm^{-1})
AMP	10.1,6.4,15.7	1.925	2.4e-5
ITCG	11.4,6.5,15.4	5.294	3.0e-5
L1LS	11.5,6.9,15.5	5.355	3.1e-5

In conclusion, we have proposed an effective reconstruction method for FMT. Numerical simulation illustrate that the proposed two-stage reconstruction enable accurate and stable recovery of the fluorescent target. In vivo mouse studies using the proposed method will be reported in the future.

REFERENCES

[1] V. Ntziachristos, J. Ripoll, L. V. Wang, and R. Weissleder, "Looking and listening to light: the evolution of whole-body photonic imaging," *Nat. Biotechnol.,* vol.23, no.3, pp.313-320, 2005.

[2] R. Weissleder, and U. Mahmood, "Molecular imaging," *Radiology*, vol.219, no.2, pp.316-333, 2001.

[3] J. K. Willmann, N. van Bruggen, L. M. Dinkelborg, and S. S. Gambhir, "Molecular imaging in drug development," *Nat. Rev. Drug Discov*. vol. 7, no.7, pp.591-607, 2008.

[4] D. Wang, X. Song, and J. Bai, "Adaptive-mesh-basd algorithm for fluorescence molecular tomography using an analytical solution," *Opt. Express*, vol.15, no.15, pp.97 22-9730, 2007.

[5] Dong Han, Jie Tian, Kai Liu, Jinchao Feng, Bo Zhang, Xibo Ma, and Chenghu Qin. Sparsity-promoting tomographic fluorescence imaging with simplified spherical harmonics approximation. IEEE Transactions on Biomedical Engineering, Vol.57, No.10, pp.2564-2567, 2010.

[6] J-C. Baritaux, K. Hassler, M.Unser. An efficient numerical method for general Lp regularization in fluorescence molecular tomography. IEEE Transactions on Medical Imaging, Vol. 29, No. 4, April 2010.

[7] H. Yi, D. Chen, X. Qu, K. Peng, X. Chen, Y. Zhou, J. Tian and Jimin Liang, "Multilevel, hybrid regularization method for reconstruction of fluorescent molecular tomography," *Appl. Opt*. vol.51, no.7, pp.975-986, 2012.

[8] D. Donoho, A. Maleki, and A. Montanari, "Message-passing algorithms for compressed sensing," PNAS, vol. 106, no. 45, pp. 18 914–18 919, 2009.

[9] A. Yang, A. Ganesh, S. Sastry, Yi Ma. Fast L1-Minimization Algorithms and An Application in Robust Face Recognition: A Review, http://www.eecs.berkeley.edu/Pubs/TechRpts/2010/EECS-2010-13.html

[10] W. Bangerth, and A. Joshi, "Adaptive finite element methods for the solution of inverse problems in optical tomography," *Inverse Probl.,* vol.24, no.3, pp.034011, 2008.

[11] M. Schweiger, S. R. Arridge, M. Hiraoka, and D. T. Delpy, "The finite element method for the propagation of light in scattering media: Boundary and source conditions," *Med. Phys*. 22, 1779–1792 (1995).

[12] W. Cong and G. Wang, "A finite-element-based reconstruction method for 3D fluorescence tomography," *Opt. Express* 13, 9847-9857(2005).

[13] P. Mohajerani, A. A. Eftekhar, J. Huang, and A. Adibi, "Optimal sparse solution for fluorescent diffuse optical tomography: theory and phantom experimental results," *Appl. Opt*., vol.46, no.10, pp.1679-1685, 2007.

[14] S. J. Kim, K. Koh, M. Lustig, S. Boyd, and D. Gorinevsky, "An Interior-Point Method for Large-Scale l1-Regularized Least Squares," IEEE Journal of Selected Topics in Signal Processing. vol. 1, no. 4, pp. 606–617, 2007.